Korean J. Chem. Eng., 37(5), 911-920 (2020)
DOI: 10.1007/s11814-020-0485-6

pISSN: 0256-1115
eISSN: 1975-7220

A monophosphonic group-functionalized ion-imprinted polymer for a removal of Fe^{3+} from highly concentrated basic chromium sulfate solution

Guang-jin Zhu*,,***, Hai-yan Tang*,**,†, Peng-hui Qing*,**, Hong-ling Zhang*,**,***, Xi-chuan Cheng****, Zai-hua Cai****, Hong-bin Xu*,**,***, and Yi Zhang*,****

*CAS Key Laboratory of Green Process and Engineering, Institute of Process Engineering, Chinese Academy of Sciences, Beijing 100190, China
**National Engineering Laboratory for Hydrometallurgical Cleaner Production Technology, Institute of Process Engineering, Chinese Academy of Sciences, Beijing 100190, China
***University of Chinese Academy of Sciences, Beijing 100049, China
****Hubei Zhenhua Chemical Co., LTD, Huangshi 435001, Hubei Province, China
(*Received 28 October 2019 • accepted 5 January 2020*)

Abstract−An ion-imprinted polymer (IIP) with monophosphonic groups was prepared by thermal copolymerization. Bis(2-methacryloxyethyl) phosphate (BMAOP) was used as functional monomer to react with Fe^{3+} in dimethyl sulfoxide (DMSO). Ethylene glycol dimethacrylate (EGDMA) was used as cross-linker during polymerization process. A suitable molar ratio of BMAOP to Fe^{3+} was investigated by UV/Vis/NIR Spectrometer and ICP-OES. The obtained results showed that the monophosphonic groups could be selectively combined with Fe^{3+} in solutions containing other coexisting ions, and the selectivity could be further enhanced by ion-imprinted process. The prepared IIP was used for removing trace Fe^{3+} from high concentration basic chromium sulfate solutions. After adsorption process, the concentration of Fe^{3+} could be reduced from 4.486 mg L^{-1} to 0.171 mg L^{-1}, which was much lower than the concentration in the solution treated by non-imprinted polymer (NIP). Moreover, the IIP exhibited excellent recyclability after six adsorption-desorption cycles.

Keywords: Ion-imprinted Polymer, Basic Chromium Sulfate, Selective Adsorption, Fe^{3+} Removal, Thermal Copolymerization

INTRODUCTION

Iron is a common impurity in chemical and hydrometallurgical industries due to its coexistence with other metals in various minerals and the wide use of iron and steel materials in industrial equipment. The presence of iron impurities seriously debases the quality of products. Thus, the removal of iron impurity in chemical or nonferrous metal products is essential to ensure high quality of products [1-3]. Basic chromium sulfate is an important chemical product which is widely applied in electroplating [4], coloring agent, printing, and leather industries [5]. Similar to other chemical products, basic chromium sulfate also contains iron impurity due to the presence of iron in its raw materials. Iron impurities in basic chromium sulfate remarkably reduce its chromium plating effects and tanning properties [6], which seriously restricts its application in electroplating and leather industries. During electroplating process, the color and plating area of the coatings will be changed due to the presence of iron impurities in trivalent chromium plating solutions [7]. In the leather industry, the tanning process is conducted through the coordination between the trivalent chromium ions in the basic chromium sulfate solutions and the carboxyl groups on the surface of leathers. However, the existence of iron impurities in tanning agents will change the color of the treated leathers due to the high reactivity between iron ions and carboxyl groups [8]. Therefore, the deep removal of iron impurity is a necessary step for the production of basic chromium sulfate. Currently, chemical precipitation is most commonly used to remove iron from the raw materials of basic chromium sulfate, containing trivalent or hexavalent chromium compounds. Phytic acid, oxalic acid, sodium dimethylaminosulfonate and other organic chelating agents are the most commonly used agents for removing iron impurities from solutions containing trivalent chromium ions. After precipitation and filtration processes, the removal rate of iron can reach 80.35% to 95.48% [9]. However, solutions containing iron precipitates produced by adding the precipitant during the chemical precipitation process have poor filterability. Solvent extraction is another method with no disadvantage of poor filtering performance. During the production of basic chromium sulfate, iron impurities are removed by using 2-ethylhexyl phosphate as the extractant. After five stage extraction and stripping, the removal rate of iron is higher than 90% [10]. However, the contamination of solutions by organic compounds and the loss of extractants cannot be ignored in the solvent extraction process due to the emulsification phenomenon. More importantly, the remaining iron concentrations in treated solutions are still higher than 10 mg L^{-1} after using the above two methods [9]. Meanwhile, iron impurities may also be introduced

†To whom correspondence should be addressed.
E-mail: hytang@ipe.ac.cn
Copyright by The Korean Institute of Chemical Engineers.

into the basic chromium sulfate product from other raw materials during the subsequent production processes. These drawbacks lead to the fact that the content of iron in the basic chromium sulfate products remains considerably high even though the iron removal operation has been conducted in the previous steps. Thus, an effective method should be found to deeply remove iron impurity from basic chromium sulfate products. Compared to the above-mentioned methods, ion exchange method, with high iron removal efficiency, lower required investment and good recyclability [11-13], has been proposed. The selectivity of the frequently used ion-exchange resins depends on their functional groups. Comparatively, ion-imprinted polymers are expected to further enhance the selectivity through the combination of functional groups and the ion-imprinting effects.

Currently, ion-imprinted polymers are often used as a new adsorbent to selectively recognize target metal ions in solutions [14-17]. They are often synthesized in a solution containing template ions through the use of cross-linker and functional monomer [18, 19]. In the copolymerization process, the bonding sites between functional groups and template ions are fixed. Then, specific sites are produced when the template is removed. These adsorption sites can selectively adsorb the target ions due to their complementarity [20]. Therefore, the IIPs are usually used to remove the target ions due to their excellent selectivity [21]. With respect to the extraction of Fe^{3+}, IIPs have exhibited excellent performance in the areas of medical [22-26], water treatment [27-30] and trace iron analysis [31,32]. High removal efficiencies have been achieved by using the Fe(III)-IIP for extracting Fe^{3+} from human plasma and various water samples which need to be purified or analyzed. However, all the above-mentioned iron removal processes are conducted in solutions containing low concentrations of coexisting ions, which may not be suitable for industrial removal of iron from high concentration basic chromium sulfate solutions. Previously, an IIP with carboxylic groups was prepared to extract Fe^{3+} from chromium nitrate solutions [33]. The results have shown that excellent iron removal performance only occurred when the content of Cr^{3+} was lower than 1.5 g L^{-1}. Meanwhile, the equilibrium adsorption time was up to 15 hours [33]. These drawbacks seriously restricted its practical application. Therefore, an IIP with the characteristics of better recognition ability and shorter equilibrium time in high concentration basic chromium sulfate solutions should be developed. Previous studies have shown that ion exchange resins with phosphonic groups exhibited good selectivity for iron in aqueous solutions [11], and the exchange resins with monophosphonic groups exhibited better performance than those with diphosphonic groups [34,35]. The iron impurities in solutions containing divalent cobalt and copper ions have been removed efficiently by the exchange resins with monophosphonic groups [11,34,35]. However, it will be more difficult to remove iron impurities from basic chromium sulfate due to the higher valence of Cr^{3+} in solutions. Compared to ion-exchange resins, the Fe(III)-IIP with monophosphonic functional groups is expected to be a suitable material to deeply remove iron impurities from high concentration basic chromium sulfate solutions due to its enhanced selectivity through ion-imprinted effect. However, no such Fe(III)-IIP has been reported so far.

In this work, an IIP with monophosphonic groups was synthesized and the molar ratio of functional monomer to Fe^{3+} was optimized. Subsequently, the adsorption behavior and the removal efficiency of Fe^{3+} were studied in high concentration basic chromium sulfate solutions.

EXPERIMENTAL

1. Reagents and Materials

Bis(2-methacryloxyethyl) phosphate (BMAOP), ethylene glycol dimethacrylate (EGDMA), $Fe(NO_3)_3{\cdot}9H_2O$, $FeCl_3{\cdot}6H_2O$ and 2,2′-azobisisobutyronitrile (AIBN) were obtained from Shanghai Aladdin Bio-Chem Technology Co., Ltd. Ethylenediaminetetraacetic acid disodium salt (Na_2EDTA), L-ascorbic acid, dimethyl sulphoxide (DMSO), $(NH_4)_2FeSO_4{\cdot}6H_2O$, KCl, $MgCl_2{\cdot}6H_2O$, $CaCl_2{\cdot}2H_2O$, $AlCl_3$, 1,10-phenanthroline monohydrate, triethylamine (Et_3N) and acetic acid (HAc) were obtained from Sinopharm Chemical Reagent Co., Ltd. H_2SO_4, NaOH and acetone were obtained from Beijing Chemical Works. Sodium acetate (NaAc) was purchased from Xilong Scientific Co., Ltd. All the above reagents were of analytical purity. Basic chromium sulfate from a foreign chemical company was used as the standard sample. Standard stock solutions (1 g L^{-1}) of chromium and iron were obtained from NCS Testing Technology Co., LTD. Deionized water was used to prepare solutions in experiments.

2. Instrumentation

Fourier transform infrared (FT-IR) spectra were obtained on a Spectrum GX FT-IR (Perkin Elmer, USA) in the range of 400-4,000 cm^{-1}. JSM-7001F scanning electronic microscopy (SEM, JEOM, Japan) was employed to analyze the morphology of polymers. An Optima 5300DV inductively coupled plasma optical emission spectrometer (ICP-OES, PerkinElmer, USA) was used to detect the concentration of phosphorus and metal ions. The surface area and pore structure of the prepared polymers were analyzed by an ASAP 2020HD88 automated adsorption apparatus (Micromeritics, USA). The pH values of solutions were measured by an FE20 digital pH meter (Metrohm, Switzerland). The UV-vis spectrophotometric measurements were performed using a Lambda 750 UV/Vis/NIR Spectrometer (Perkin Elmer, USA).

3. Preparation of IIP and NIP

First, 3 mmol of BMAOP and 3 mmol of Et_3N were added to 10 mL of DMSO and stirred for 0.5 h. The complex between functional monomer and template ions was formed by adding 1 mmol of $Fe(NO_3)_3{\cdot}9H_2O$ to the above solution and stirred for 2 h, and then 0.04 g of AIBN and 16 mmol of EGDMA were added. After being stirred for a moment, the O_2 was removed from the system by purging with N_2. Subsequently, the obtained mixture was heated at 60 °C for 24 h. Then the prepared polymer was crushed and sieved and particles with diameters of 180-450 μm were obtained. The template ions in the obtained particles were leached by Na_2EDTA solution for six times and then leached by the solutions of NaOH, HCl and Na_2EDTA in turn. The concentrations of Na_2EDTA, NaOH and HCl solutions were 0.1 mol L^{-1}, 2.5 mol L^{-1} and 6 mol L^{-1}, respectively. Finally, the particles were washed with acetone and water in turn. The water remaining in polymers was removed by heating at 60 °C. Similarly, the NIP was synthesized without using the template ions.

4. Adsorption Experiments

The measurement of the adsorption performance of the pre-

pared polymers was conducted in the synthetic solution containing 50 mg L^{-1} of Fe^{3+} and 30 g L^{-1} of basic chromium sulfate. 0.02 g of polymers was added to 10 mL of the above solution to study the suitable pH value and adsorption time, as well as the adsorption kinetics and the recyclability of the polymers. Moreover, the maximum adsorption capacity and adsorption equilibrium were also studied in synthetic basic chromium sulfate solutions containing 15-130 mg L^{-1} of Fe^{3+}. The mass ratio of iron to basic chromium sulfate in the solutions was maintained at about 1 : 600.

The adsorption capacity of prepared polymers and the iron removal rate in solutions were calculated in terms of Eqs. (1) and (2):

$$q = \frac{(c_0 - c_e)V}{m} \quad (1)$$

$$R = \frac{c_0 - c_e}{c_0} \quad (2)$$

The selectivity of prepared polymers was studied in mixtures containing 30 mg L^{-1} of binary metal ions. 0.02 g of polymers were added to 10 mL of the mixtures to determination the adsorption ability of polymers for Fe^{3+} in the presence of Cr^{3+}, Co^{2+}, Ni^{2+}, Cu^{2+} or Zn^{2+}, respectively. The distribution coefficient and the selectivity parameters were calculated in terms of the following equations [36]:

$$D = \frac{(c_0 - c_e)V}{c_e m} \quad (3)$$

$$k = \frac{D_{Fe}}{D_M} \quad (4)$$

$$k' = \frac{k_{IIP}}{k_{NIP}} \quad (5)$$

The iron removal efficiency of IIP and NIP in basic chromium sulfate solutions was investigated. Synthetic solution was prepared which contained 4-4.5 mg L^{-1} of Fe^{3+} and 30 g L^{-1} of basic chromium sulfate. 0.02 g of the prepared polymers was added to 10 mL of the above solutions to remove of Fe^{3+}. The effect of coexisting ions was also investigated under similar adsorption conditions.

All above-mentioned experiments were conducted at 25 °C in a shaking table with a shaking speed of 250 r min^{-1}. All the pH values were adjusted by H_2SO_4 or NaOH solutions. All experiments were conducted at least three times in parallel.

RESULTS AND DISCUSSION

1. Optimization of the Molar Ratio of Functional Monomer to Fe^{3+}

The content of functional monomer has a significant effect on the performance of IIPs. Insufficient functional monomer will make it difficult for its formation of compound with template ions. However, numerous non-imprinted adsorption sites will be formed when its content is superfluous [37]. Thus, a suitable molar ratio of BMAOP to Fe^{3+} must be confirmed before the synthesis of the IIP.

First, UV-vis spectrophotometric measurements were performed to determine the suitable content of BMAOP. $FeCl_3 \cdot 6H_2O$ was chosen as the source of Fe^{3+} due to its better solubility in DMSO. As can be seen in Fig. 1, two peaks appeared in the UV-vis spectrum of free $FeCl_3$ at the wavelengths of 258 nm and 337 nm, respectively. With the increase of the content of BMAOP in solutions, the intensity of characteristic peaks of $FeCl_3$ decreased gradually, indicating the reaction process was conducted between BMAOP and Fe^{3+}. According to the relationship between the c(BMAOP)/c(Fe^{3+}) and the absorbance at the wavelength of 337 nm, the absorbance decreased sharply when the molar ratio shifted from 0 : 1 to 3 : 1, which indicated an inadequate content of BMAOP relative to Fe^{3+}. A much slower decrease of absorbance occurred when the molar ratio continued to increase, suggesting that the content of BMAOP was superfluous. It indicated that a complex compound with BMAOP/Fe^{3+} molar ratio of 3 : 1 was formed.

Moreover, the complex compound of BMAOP with Fe^{3+} was synthesized and the P/Fe ratio of the compound was detected. First, 1 mmol of $Fe(NO_3)_3 \cdot 9H_2O$, 3 mmol of BMAOP and 3 mmol of Et_3N were added to 10 mL of DMSO to form a compound. Then, deionized water was poured in the mixture to produce the precipitates. After filtering and drying process, the precipitates were digested

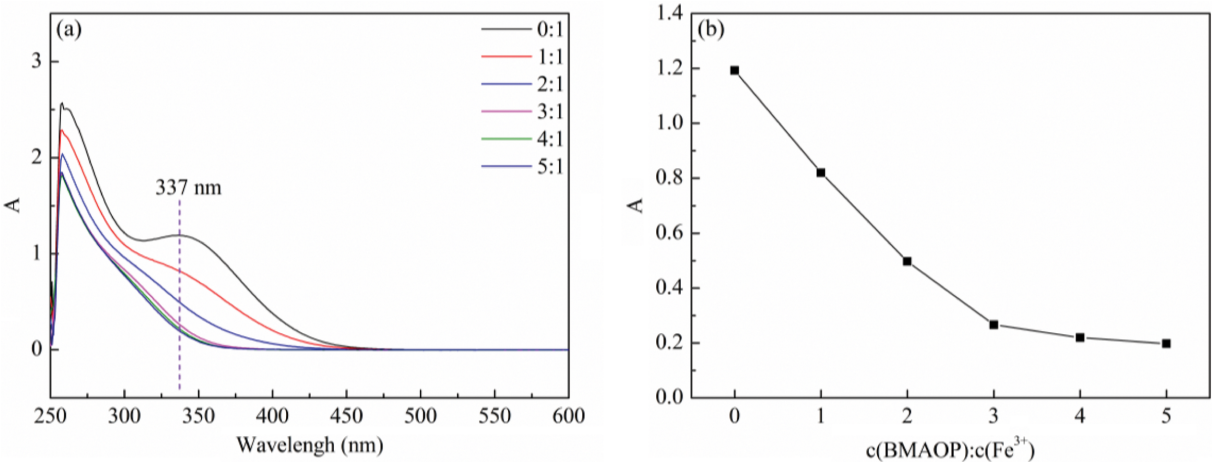


Fig. 1. UV-vis spectral analysis of different molar ratio of BMAOP to $FeCl_3$ in DMSO: (a) UV-vis spectrum; (b) the relationship between absorbance and c(BMAOP)/c(Fe^{3+}) at the wavelength of 337 nm.

by aqua regia. The content of phosphorus and iron was detected by ICP-OES and the results showed that the molar ratio of phosphorus to iron of the compound was 2.96 : 1 which was close to 3 : 1, indicating that a 3 : 1 complex compound was formed. According to the above results, the molar ratio of BMAOP to Fe^{3+} was determined to 3 : 1 during the synthetic process.

2. Characterizations of IIP and NIP

The prepared polymers were analyzed by FT-IR spectrometer. The results are presented in Fig. 2. The similar backbones of the spectra of IIP and NIP were due to their similar composition. There were two strong peaks at 1,261 cm^{-1} and 1,159 cm^{-1} in the spectra of IIP and NIP, which are the characteristic peaks of P=O group. The stretching vibration peak of O=P-O- in NIP appeared at 1,069 cm^{-1}, which appeared at 1,064 cm^{-1} in IIP. The different frequencies for O=P-O- band in IIP and NIP were due to the combination between Fe^{3+} and BMAOP in IIP. The results demonstrated that the functional groups had been produced in polymers and the imprinting process was successfully completed.

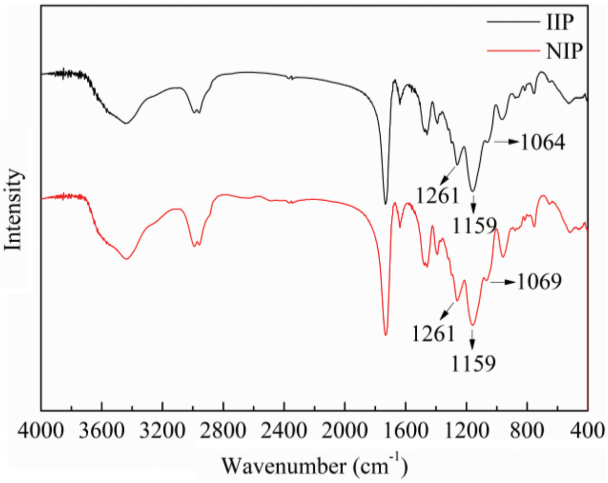


Fig. 2. FT-IR spectra of the prepared IIP and NIP.

According to the above results, the formation of IIP is presented in Fig. 3. First, a complex compound with BMAOP/Fe^{3+} molar ratio of 3 : 1 was formed and then copolymerized with EGDMA. After that, the interaction sites were fixed in the polymer. Finally, the Fe^{3+} was removed to form the special sites.

SEM was used to analyze the morphology of the prepared polymers. The results in Fig. 4 indicate that the surface morphology of IIP and NIP was rough. Meanwhile, it seems that numerous pores existed in the prepared polymers. That structure might be attributed to the pore-forming action of DMSO during the synthetic process [38]. The mapping results of the prepared IIP imprinted with ferric ions showed that the elements of phosphorus and iron were homogeneously distributed throughout the whole polymer. The atomic ratio of phosphorus to iron was close to 3 : 1, which is consistent with the previous analysis results.

N_2 adsorption/desorption isotherms were used to characterize the surface area and pores of the synthesized IIP and NIP. The BET and BJH theory were employed to calculate the surface area and

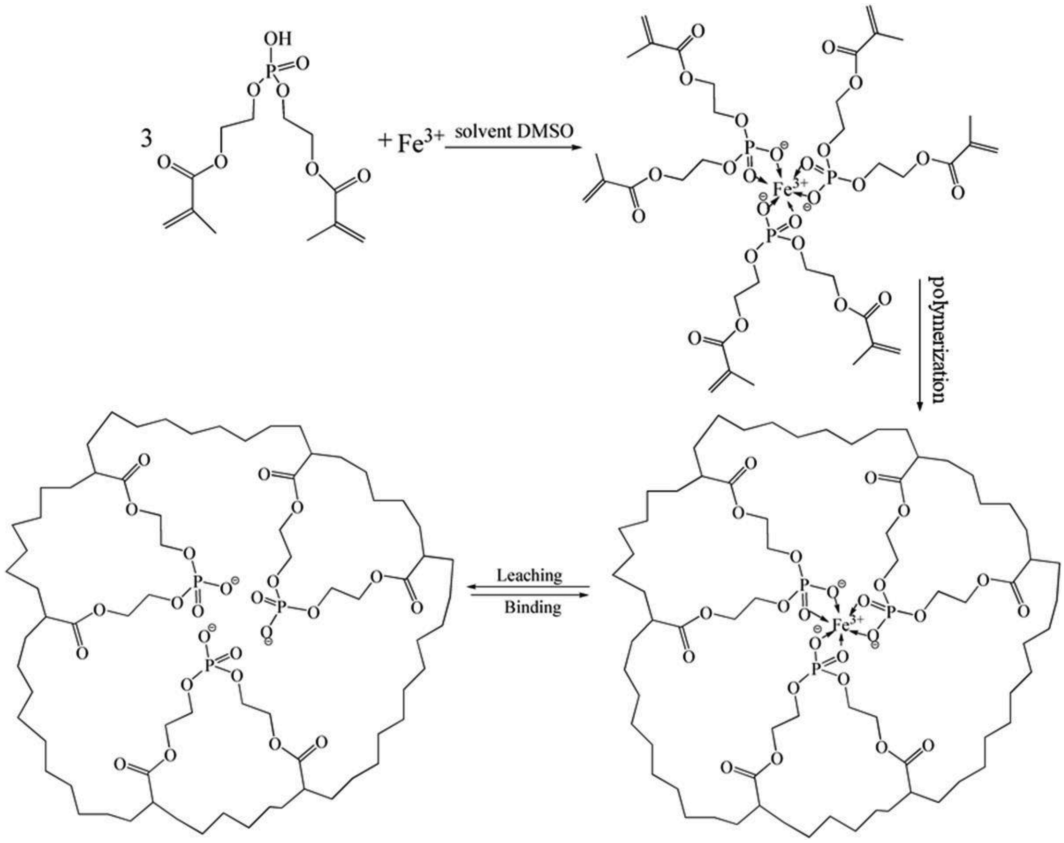


Fig. 3. Scheme for the preparation of IIP.

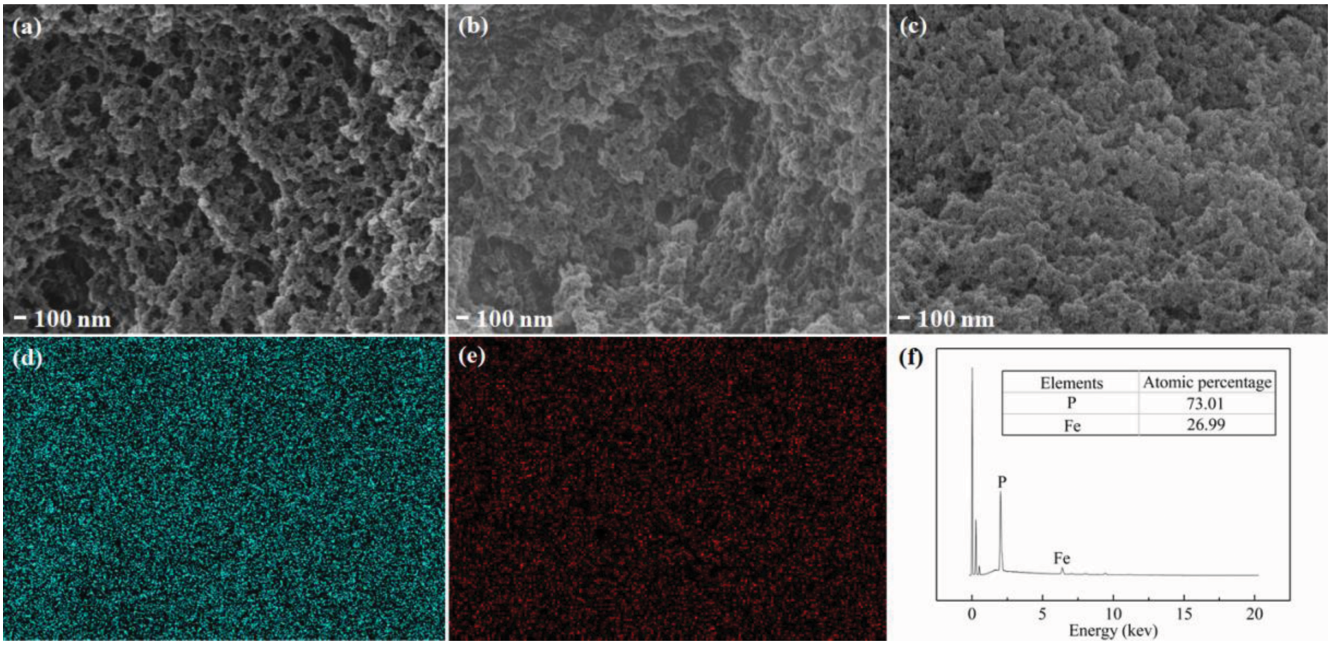


Fig. 4. SEM images of the prepared polymers: (a) IIP imprinted with ferric ions; (b) leached IIP; (c) NIP; (d) mapping results of phosphorus for IIP imprinted with ferric ions; (e) mapping results of iron for IIP imprinted with ferric ions; (f) spectrum of mapping results.

the pore diameter/volume, respectively. The results showed that the surface area, pore diameter and pore volume of IIP were 233.96 $m^2 g^{-1}$, 10.629 nm and 0.680 $cm^3 g^{-1}$, respectively. With respect to NIP, the corresponding properties were 275.86 $m^2 g^{-1}$, 9.256 nm and 0.705 $cm^3 g^{-1}$, respectively. It could be found that the polymers had large surface areas, which might be due to the pore-forming action of DMSO. When the DMSO was washed from the polymers, the large surface areas were generated because of the excellent thermodynamic compatibility of DMSO for the polymers during the polymerization process [38].

3. The Adsorption Ability of IIP and NIP in Basic Chromium Sulfate Solutions

3-1. The Determination of Suitable pH Value

The pH value can significantly affect the adsorption capacity due to the easy hydrolysis of iron ions. The Fe^{3+} can combine with OH^- in various forms at different pH values [39,40], which may affect the adsorption ability of IIP or NIP [33]. Meanwhile, a reduction of adsorption capacity may occur due to the occupation of bonding sites by H^+ at low pH values. Therefore, a suitable pH value should be confirmed.

The experiments were carried out in basic chromium sulfate solutions adsorbing for 6 h under different pH values. From the results in Fig. 5, the low adsorption capacities at pH value of 1.0 were due to protonation. When the pH value increased continually, the adsorption capacities increased sharply. Relatively large adsorption capacities appeared at pH value between 2.0 and 3.0. When the pH value continued to increase, the adsorption capacities decreased due to the formation of hydroxide in solution. Thus, the suitable pH value was 2.0-3.0. Therefore, the pH value of 2.0 was chosen in the subsequent experiments. In addition, at all the pH values which were chosen in these experiments, it could be found that the IIP had better adsorption ability than the NIP, indicating that the imprinting process had a great influence on the performance of IIP.

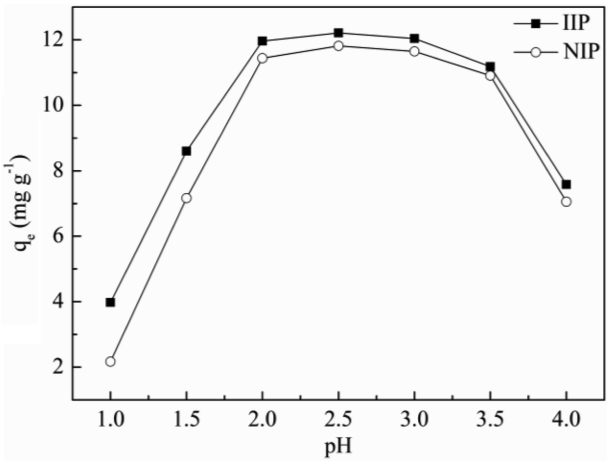


Fig. 5. The adsorption capacities of IIP and NIP at different initial pH values.

3-2. Adsorption Isotherm in Basic Chromium Sulfate Solutions

The adsorption capacity, which determines the amount of adsorbents required, is an important property for the prepared polymers. The related adsorption experiments were performed under incremental initial concentrations of Fe^{3+} and basic chromium sulfate at the pH value of 2.0 adsorbing for 6.0 h. The results in Fig. 6 show that when the initial concentration was increased, the adsorption capacities became larger at the beginning and then leveled off. The maximum adsorption capacity of IIP and NIP in basic chromium sulfate solutions was 15.71 mg g^{-1} and 14.72 mg g^{-1}, respectively. Meanwhile, the maximum values occurred when the

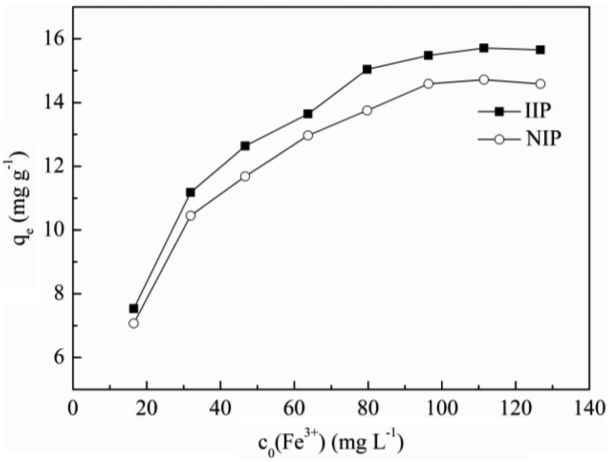


Fig. 6. The adsorption capacities of IIP and NIP at different initial concentrations of Fe^{3+}.

concentration of basic chromium sulfate was as high as 63 g L^{-1} and no obvious decrease was observed as the concentration increased continually, indicating that the prepared polymers exhibited an excellent adsorption ability for Fe^{3+} in high concentration basic chromium sulfate solutions.

The adsorption isotherm was calculated through the Langmuir and Freundlich models. These two models could be described as follows [12]:

$$\text{Langmuir model: } \frac{c_e}{q_e} = \frac{1}{q_m K_L} + \frac{c_e}{q_m} \quad (6)$$

$$\text{Freundlich model: } \ln q_e = \frac{1}{n}\ln c_e + \ln K_F \quad (7)$$

The linearized adsorption isotherms are provided in Fig. 7 and the corresponding parameters are listed in Table 1. The results show that the Freundlich model was more suitable to describe the adsorption behavior of IIP and NIP. The values of R^2 of IIP and NIP for Freundlich model were 0.994 and 0.991, respectively, while the corresponding values for Langmuir model were only 0.909 and 0.936. The values of Freundlich parameter (1/n) were between 0 and 1, indicating favorable adsorption abilities of IIP and NIP for Fe^{3+} [41].

3-3. Adsorption Kinetics in Basic Chromium Sulfate Solutions

The equilibration adsorption times of IIP and NIP in basic chromium sulfate solutions were investigated by changing the adsorption time from 5 min to 6 h. The results in Fig. 8 show that the adsorption capacity increased obviously within the first 2 hours and

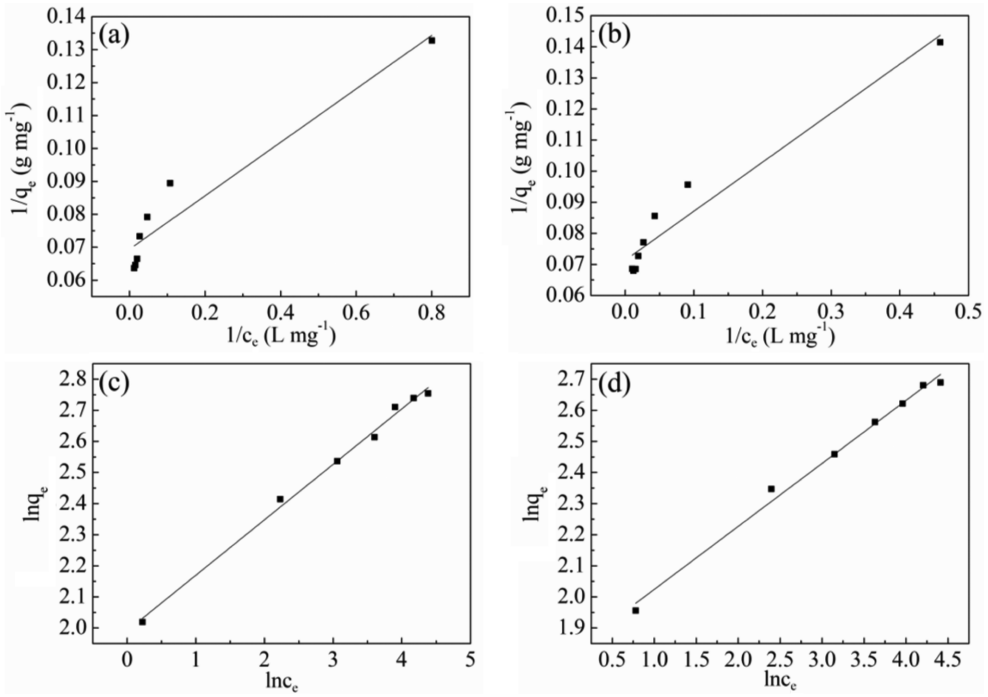


Fig. 7. Fitting curves of Langmuir and Freundlich models: (a) Langmuir isotherm of IIP; (b) Langmuir isotherm of NIP; (c) Freundlich isotherm of IIP; (d) Freundlich isotherm of NIP.

Table 1. Langmuir and Freundlich isotherms parameters of IIP and NIP

Models	Langmuir			Freundlich		
Parameters	q_m (mg g^{-1})	K_L (L mg^{-1})	R^2	1/n	lnK_F	R^2
IIP	14.41	0.856	0.909	0.178	1.991	0.994
NIP	14.01	0.453	0.936	0.202	1.822	0.991

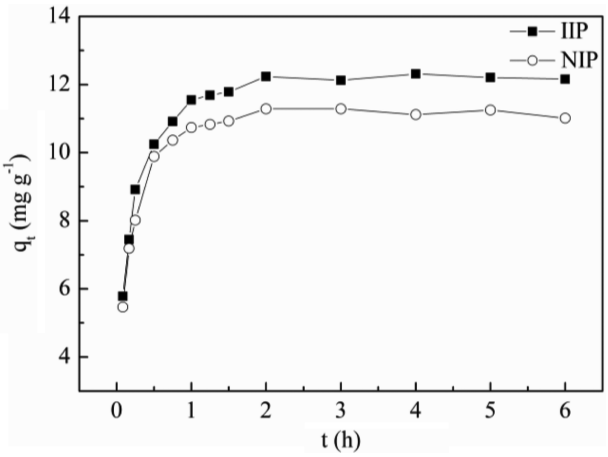


Fig. 8. The adsorption capacities of IIP and NIP at different adsorption time.

then reached a constant level. Thus, the equilibration time was determined as 2 h, which was much shorter than the IIP with carboxylic groups adsorbing Fe^{3+} in Cr^{3+}-containing solutions [33]. Therefore, the adsorption time of 3 h was used in subsequent experiments to ensure the equilibrium of adsorption.

The adsorption kinetics was calculated through the pseudo-first-order models and pseudo-second-order models. These two models could be described as follows [41]:

$$\text{Pseudo-first-order model: } \ln(q_e - q_t) = \ln q_e - k_1 t \quad (8)$$

$$\text{Pseudo-second-order model: } \frac{1}{q_t} = \frac{1}{k_2 q_e^2 t} + \frac{1}{q_e} \quad (9)$$

The linear fitting results of kinetics models are shown in Fig. 9, indicating that the adsorption behavior of IIP and NIP tallied with pseudo-second-order kinetics. The corresponding parameters in Table 2 indicate that the q_e of IIP and NIP obtained from the fitting results of pseudo-second-order model were closer to the data obtained from the experiments (12.48 mg L^{-1} for IIP and 11.62 mg L^{-1} for NIP). The values of R^2 of pseudo-second-order kinetics were 0.991 for IIP and 0.992 for NIP, respectively, while the corresponding data of pseudo-first-order model were only 0.960 and 0.940. Therefore, the adsorption of Fe^{3+} might be a chemical process [42].

The Weber-Morris model was used to estimate the diffusion behavior during the adsorption process. The model could be described as follows [43]:

$$q_t = K_{dif} t^{1/2} + C \quad (10)$$

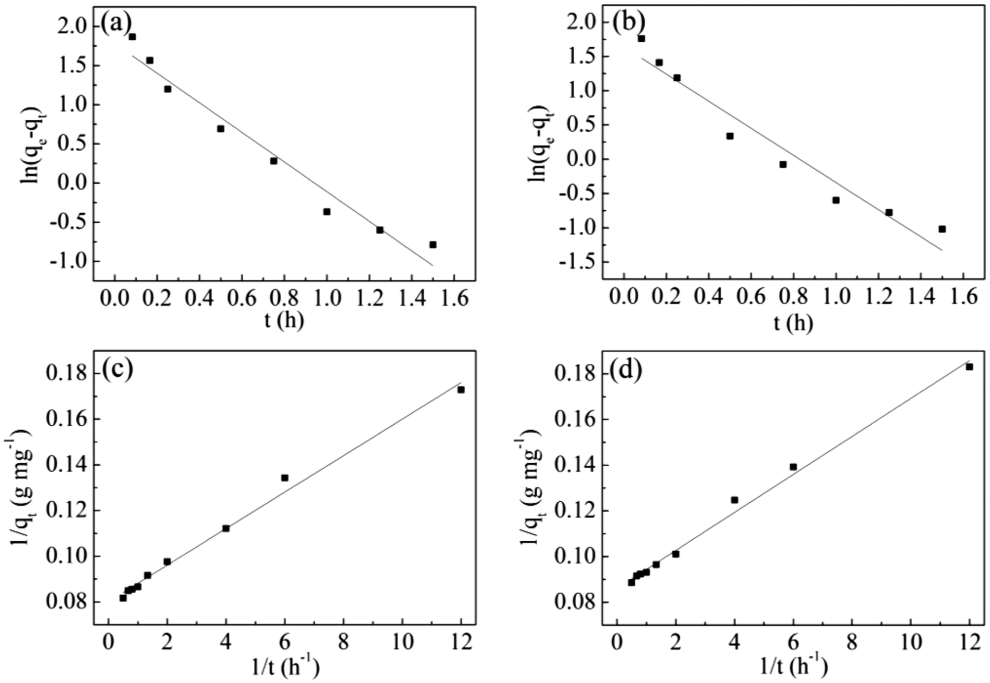


Fig. 9. Linearized pseudo-first-order and pseudo-second-order models: (a) Pseudo-first-order model for IIP; (b) pseudo-first-order model for NIP; (c) pseudo-second-order model for IIP; (d) pseudo-second-order model for NIP.

Table 2. Pseudo-first-order and pseudo-second-order kinetics parameters of IIP and NIP

Models	Pseudo-first-order			Pseudo-second-order		
Parameters	q_e (mg·g^{-1})	k_1 (h^{-1})	R^2	q_e (mg·g^{-1})	k_2 (g mg^{-1} h^{-1})	R^2
IIP	5.935	1.892	0.960	12.48	0.804	0.991
NIP	5.143	1.978	0.940	11.62	0.891	0.992

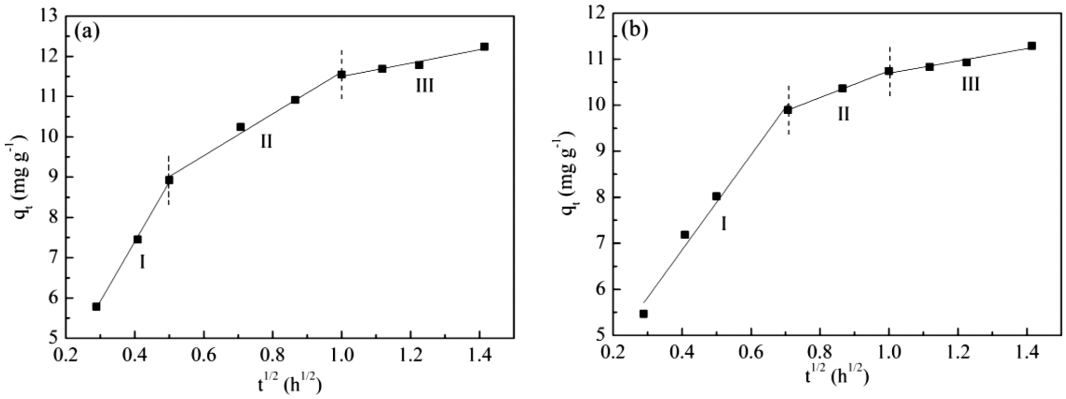


Fig. 10. Weber-Morris model plots for the adsorption of Fe^{3+} onto IIP (a) and NIP (b).

Table 3. Selectivity parameters of IIP and NIP

Binary ions	IIP			NIP			k′
	D_{Fe}	D_M	k	D_{Fe}	D_M	k	
Fe^{3+}/Cr^{3+}	5.97	8.51×10^{-3}	701.10	3.95	13.73×10^{-3}	287.53	2.44
Fe^{3+}/Co^{2+}	4.17	0.60×10^{-3}	6925.99	3.37	8.51×10^{-3}	1579.98	4.38
Fe^{3+}/Ni^{2+}	8.40	6.45×10^{-3}	1302.12	4.26	13.65×10^{-3}	312.50	4.17
Fe^{3+}/Cu^{2+}	4.87	4.16×10^{-3}	1171.43	3.76	5.72×10^{-3}	658.23	1.78
Fe^{3+}/Zn^{2+}	7.00	2.57×10^{-3}	2726.39	4.50	6.86×10^{-3}	656.69	4.15

Theoretically, the plots of this model usually present multi-linearity, indicating that there are several steps during the adsorption process [44,45]. Similar results were achieved during the adsorption of Fe^{3+} onto the prepared polymers. It could be found from Fig. 10 that the diffusion process could be dissociated into three stages. An external surface adsorption process occurred in the first stage due to the high initial concentration difference [46]. Compared with the NIP, the second stage for Fe^{3+} adsorbing onto the IIP, which could be determined as an intraparticle diffusion process [47], was started in shorter adsorption time. After that, an equilibrium process could be used to describe the third stage. The diffusion rate slowed and the adsorption began to reach saturation. The linear lines were not passing through the original point, indicating that the intraparticle diffusion was not the only rate controlling step [47].

4. Adsorption Selectivity

The selective adsorption experiments were conducted in binary mixtures containing Fe^{3+} and coexisting ions (Cr^{3+}, Co^{2+}, Ni^{2+}, Cu^{2+} or Zn^{2+}) since the above ions have similar chemical properties to Fe^{3+}. In Table 3, the distribution coefficients of NIP for Fe^{3+} were much greater than those for coexisting ions, resulting in the high selectivity coefficients of NIP, which demonstrated that the monophosphonic groups itself had good selectivity for Fe^{3+}. The selectivity coefficients of IIP were much higher than that of NIP, indicating that the selectivity was further enhanced by the ion-imprinting process. Furthermore, the relative selectivity coefficients, which represent the selectivity of the IIP relative to the NIP, were not too high. That was because the high-selective monophosphonic groups led to a high value of k_{NIP} and then resulted in a low ratio of k_{IIP} to k_{NIP}. Even so, the values of relative selectivity coefficients were still higher than 1, indicating that the ion-imprinting process was conducted successfully.

5. Desorption and Regeneration of IIP and NIP

The recyclability of the prepared polymers is an important factor for industrial application. The adsorbed Fe^{3+} and Cr^{3+} ions were eluted by Na_2EDTA solution and NaOH solution, respectively. The adsorption-desorption cycles were performed for six times. After adsorption and desorption process, the polymers were recovered by filtration and then dried at 60 °C. The pore size of the microporous membrane used in the filtration process was 0.22 μm. The slight loss of the polymers during the recovering process was supplemented by the additional parallel experiments. As seen in Fig. 11, the adsorption capacities of IIP and NIP had no obvious de-

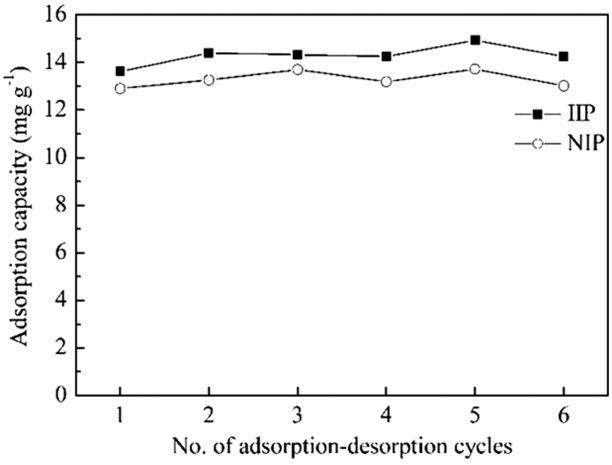


Fig. 11. Desorption and regeneration of IIP and NIP.

Table 4. Removal efficiencies and concentration change of Fe^{3+} and Na^{+} ions

Polymers	Ion species	Concentration in initial solutions (mg L^{-1})	Concentration in treated solution (mg L^{-1})	Removal rate (%)
IIP	Fe^{3+}	4.486	0.171	96.19
	Na^{+}	2438	2444	——
NIP	Fe^{3+}	4.486	0.316	92.95
	Na^{+}	2438	2442	——

crease after six cycles, indicating their excellent recyclability.

6. The Removal of Fe^{3+} from Basic Chromium Sulfate Solutions

After the determination of suitable adsorption conditions, Fe^{3+} was removed from basic chromium sulfate solutions by IIP and NIP under the obtained suitable conditions. The results in Table 4 indicate that the remaining Fe^{3+} in solution treated by IIP could be as low as 0.171 mg L^{-1}, while the corresponding concentration in solution treated by NIP was 0.316 mg L^{-1}, which was 1.85-times higher than that of concentration in solution treated by IIP. This difference indicated that the ion imprinted process was a key factor which affected the adsorption property of IIP. Since the presence of template ions, the functional groups were fixed in an orderly manner in the polymerization process. After the template removal process, the specific binding sites and imprinted cavities were formed and then the imprinting process was completed. However, no such process was conducted in the preparation of NIP [48]. Moreover, it could be found that numerous of Na^{+} existed in basic chromium sulfate and the removal rate of Fe^{3+} could be maintained at a high level in the presence of Na^{+}.

The effects of other impurities in basic chromium sulfate on removal efficiencies were also investigated under the obtained suitable conditions. The metal ions of K^{+}, Mg^{2+}, Ca^{2+} or Al^{3+} were added to the synthetic solutions, respectively, to ensure the concentrations of coexisting ions were maintained at 20-27 mg L^{-1}. The results are presented in Table 5. It can be seen that there was nearly no decrease of iron removal rate at the existence of K^{+}, Ca^{2+} and Mg^{2+}, and a slight decrease occurred at the existence of Al^{3+}. That might be due to the occupation of adsorption sites by Al^{3+}. The removal rate of Al^{3+} was as high as 17.85%, which was much higher than the removal rates of Ca^{2+} (4.10%), Mg^{2+} (1.11%) and K^{+} (0.08%), indicating that the coexisting ions with high valence were more easily adsorbed on IIP.

CONCLUSIONS

An Fe(III)-IIP was synthesized and applied for the removal of Fe^{3+} from high concentration basic chromium sulfate solutions. The main conclusions are listed below:

(1) BMAOP was an excellent functional monomer to prepare IIP with good selectivity for Fe^{3+}. The suitable molar ratio of BMAOP to Fe^{3+} was 3 : 1.

(2) A high adsorption capacity was obtained at initial pH value of 2.0 and adsorbed for 3 h. The adsorption isotherm and kinetics of IIP and NIP followed the Freundlich model and the pseudo-second-order model, respectively. Moreover, no obvious decrease of adsorption capacity occurred after six adsorption-desorption cycles.

(3) After adsorption process, the concentration of Fe^{3+} could be reduced from 4.486 mg L^{-1} to 0.171 mg L^{-1}, which was much lower than the concentration in the solution treated by NIP.

ACKNOWLEDGEMENTS

This research was supported by the China National Major Science and Technology Program for Water Pollution Control and Treatment (Grant NO. 2018ZX07402005).

NOMENCLATURE

c_0 : initial concentration [mg L^{-1}]
c_e : equilibrium concentration [mg L^{-1}]
D : distribution ratio [mL g^{-1}]
k : selectivity coefficient
k_1 : kinetics constant [h^{-1}]
k_2 : kinetics constant [g mg^{-1} h^{-1}]
k′ : relative selectivity coefficient

Table 5. Removal efficiencies of Fe^{3+} at the existence of different common ions

No.	Ion species	Concentration in initial solutions (mg L^{-1})	Concentration in treated solution (mg L^{-1})	Removal rate (%)
1	Fe^{3+}	4.419	0.184	95.84
	K^{+}	23.80	23.78	0.08
2	Fe^{3+}	4.404	0.159	96.40
	Ca^{2+}	26.82	25.72	4.10
3	Fe^{3+}	4.452	0.181	95.94
	Mg^{2+}	25.24	24.96	1.11
4	Fe^{3+}	4.367	0.286	93.46
	Al^{3+}	21.18	17.40	17.85

K_F, 1/n : Freundlich constants
K_L : Langmuir constant [L mg^{-1}]
m : mass of polymers [g]
q : adsorption capacity [mg g^{-1}]
q_e : equilibrium adsorption capacity [mg g^{-1}]
q_m : maximum adsorption capacity [mg g^{-1}]
q_t : adsorption capacity at the time of t [mg g^{-1}]
R : removal rate
V : volume of solutions [L]
K_{dif} : intraparticle diffusion rate constant [mg g^{-1} $min^{-1/2}$]
C : intercept Weber-Morris equation [mg g^{-1}]

REFERENCES

1. Y. Ma, X. Wang, M. Wang, C. Jiang, X. Xiang and X. Zhang, *Hydrometallurgy*, **153**, 38 (2015).
2. G. Hu, D. Chen, L. Wang, J. Liu, H. Zhao, Y. Liu, T. Qi, C. Zhang and P. Yu, *Sep. Purif. Technol.*, **125**, 59 (2014).
3. X. Yang, Y. Zhang, S. Bao and C. Shen, *Sep. Purif. Technol.*, **164**, 49 (2016).
4. H. Mei, G. Li, K. Wang and X. Li, *Inorg. Chem. Ind. (In Chinese)*, **34**, 34 (2002).
5. H. Weng, *Chem. World (In Chinese)*, **35**, 50 (1994).
6. A. Liu and L. Jia, *Chin. Leather (In Chinese)*, **36**, 26 (2007).
7. C. Guo and S. Yi, *Plat. Finish. (In Chinese)*, **30**, 28 (2008).
8. X. Chen, *Chin. Leather (In Chinese)*, **38**, 1 (2009).
9. X. Chen, *Inorg. Chem. Ind. (In Chinese)*, **46**, 13 (2014).
10. X. Li, N. Chen, G. Zhang, L. Qin and T. Yin, *Chrom. Ind. (In Chinese)*, **1**, 48 (2010).
11. G. Wang, Y. Zhao, B. Yang and Y. Song, *Hydrometallurgy*, **176**, 69 (2018).
12. Y. Zhang, X. Zhou, Z. Liu, B. Li, Q. Liu and X. Li, *Rsc Adv.*, **6**, 6695 (2016).
13. M. S. Lee and M. J. Nicol, *Hydrometallurgy*, **86**, 6 (2007).
14. H. Nishide, J. Deguchi and E. Tsuchida, *Chem. Lett.*, **5**, 169 (1976).
15. E. Birlik, A. Ersoz, E. Acikkalp, A. Denizli and R. Say, *J. Hazard. Mater.*, **140**, 110 (2007).
16. C. Branger, W. Meouche and A. Margaillan, *React. Funct. Polym.*, **73**, 859 (2013).
17. Ö. Saatçılar, N. Şatıroğlu, R. Say, S. Bekta and A. Denizli, *J. Appl. Polym. Sci.*, **101**, 3520 (2006).
18. J. Fu, L. Chen, J. Li and Z. Zhang, *J. Mater. Chem. A*, **3**, 13598 (2015).
19. H. Liang, Q. Chen and X. Shen, *J. Nucl. Radiochem.*, **38**, 129 (2016).
20. M. Randhawa, I. Gartner, C. Becker, J. Student, M. Chai and A. Mueller, *J. Appl. Polym. Sci.*, **106**, 3321 (2007).
21. A. H. Dam and D. J. Kim, *J. Appl. Polym. Sci.*, **108**, 14 (2008).
22. S. Aslıyüce, N. Bereli, L. Uzun, M. A. Onur, R. Say and A. Denizli, *Sep. Purif. Technol.*, **73**, 243 (2010).
23. D. Cimen, I. Gokturk and F. Yilmaz, *Artif. Cells Nanomed. Biotechnol.*, **44**, 1158 (2016).
24. B. Ergün, G. Baydemir, M. Andaç, H. Yavuz and A. Denizli, *J. Appl. Polym. Sci.*, **125**, 254 (2012).
25. S. Özkara, R. Say, C. Andaç and A. Denizli, *Ind. Eng. Chem. Res.*, **47**, 7849 (2008).
26. H. Yavuz, R. Say and A. Denizli, *Mater. Sci. Eng. C*, **25**, 521 (2005).
27. H. T. Fan and T. Sun, *Korean J. Chem. Eng.*, **29**, 798 (2012).
28. M. Khajeh, M. Kaykhaii, H. Hashemi and M. Mirmoghaddam, *Polym. Sci. Ser. B*, **51**, 344 (2009).
29. S. Özkara, M. Andaç, V. Karakoç, R. Say and A. Denizli, *J. Appl. Polym. Sci.*, **120**, 1829 (2011).
30. D. K. Singh and S. Mishra, *J. Sci. Ind. Res.*, **69**, 767 (2010).
31. M. Roushani, T. M. Beygi and Z. Saedi, *Spectrochim. Acta. Mol. Biomol. Spectros.*, **153**, 637 (2016).
32. X. Chang, N. Jiang, H. Zheng, Q. He, Z. Hu, Y. Zhai and Y. Cui, *Talanta*, **71**, 38 (2007).
33. G.-j. Zhu, H.-y. Tang, H.-l. Zhang, L.-l. Pei, P. Zhou, Y.-l. Shi, Z.-h. Cai, H.-b. Xu and Y. Zhang, *Hydrometallurgy*, **186**, 105 (2019).
34. B. McKevitt and D. Dreisinger, *Hydrometallurgy*, **98**, 122 (2009).
35. B. McKevitt and D. Dreisinger, *Hydrometallurgy*, **98**, 116 (2009).
36. H. He, Q. Gan and C. Feng, *J. Appl. Polym. Sci.*, **134**, 45165 (2017).
37. M. Komiyama, T. Takeuchi, T. Mukawa and H. Asanuma, *Molecular imprinting: from fundamentals to applications*, Sci. Press, Beijing (2003).
38. H. L. Liang, Q. D. Chen, J. Y. Ma, Y. Y. Huang and X. H. Shen, *Rsc Adv.*, **7**, 35394 (2017).
39. J. Formanek, J. Jandova and J. Capek, *Hydrometallurgy*, **138**, 100 (2013).
40. Y. A. El-Nadi and N. E. E-Hefny, *Chem. Eng. Process.*, **49**, 159 (2010).
41. P. Li, S. L. Zheng, P. H. Qing, Y. G. Chen, L. Tian, X. D. Zheng and Y. Zhang, *Green Chem.*, **16**, 4214 (2014).
42. M. Parijaee, M. Noaparast, K. Saberyan and S. Z. Shafaie-Tonkaboni, *Korean J. Chem. Eng.*, **31**, 2237 (2014).
43. W. Weber and J. Morris, *J. Sanit. Eng. Div. Am. Soc. Civ. Eng.*, **89**, 31 (1963).
44. B. H. Hameed, I. A. W. Tan and A. L. Ahmad, *Chem. Eng. J.*, **144**, 235 (2008).
45. R. S. Juang, F. C. Wu and R. L. Tseng, *J. Colloid Interface Sci.*, **227**, 437 (2000).
46. J. B. Zhou, L. Wang, Z. Zhang and J. G. Yu, *J. Colloid Interface Sci.*, **394**, 509 (2013).
47. X. Chen, J. Pan and Y. Yan, *Acta Phys.-Chim. Sin.*, **32**, 2794 (2016).
48. Z. Li, W. Kou, S. Wu and L. Wu, *Anal. Methods*, **9**, 3221 (2017).